Morphological, Thermal and Mechanical Properties of Epoxidized Soil Bean Plasticized Polylactic Acid/Graphene Nanocomposites

Buncha Suksut[1]*, Thanyamas Huayhongtong [1], Kanokwon Mangkang [1], Weerapat Saisuwan [1]

[1]Materials and Process Engineering Technology, Faculty of Engineering and Technology,
King Mongkut's University of Technology North Bangkok Rayong Campus
* E-mail: buncha.s@eat.kmutnb.ac.th

Abstract

Due to their biodegradability, both polylactic acid (PLA) and epoxidized soil bean (ESO) were blended at various contents of ESO (3-10 wt%) by melt blending in an internal mixer. Inclusion of 10 wt% of ESO into PLA showed the highest elongation at break and the impact strength. The incorporation of graphene (GP) into PLA/ESO blend promoted the impact strength of the composites accompanied by lowering stiffness and strength. From DSC analysis, the glass transition temperature (T_g) decreased, while the degree of crystallinity of PLA increased with the inclusion of ESO. Crystallization temperature (T_c) of PLA at 10 wt% of ESO decreased about 10°C in comparison with neat PLA. However, the presence of GP has no significant effect on any transition temperatures of PLA, but led to smaller spherulite size. The resulting performances of the plasticized PLA composite were explained by two possibilities, the interfacial adhesion between PLA matrix and GP particles as well as the competitive effect of ESO and GP on PLA crystallization.

Keywords: biopolymer, bioplasticizer, graphene, crystallization

Introduction

Biopolymers have been receiving a great attention as the potential and useful replacement of petroleum based polymers as a result of rising concerns about the environment, energy and sustainability. Polylactic acid is one of the most promising candidates for biopolymers due to its renewable resources, abundance and easy availability (Meng et al., 2018). PLA provides a relatively easy processability, high strength and high stiffness. However, a broader application of PLA is hindered by its mechanical brittleness, low heat distortion temperature, slow crystallization rate and relative high cost (Al-Mulla, Suhail & Aowda, 2011; Meng et al., 2018).

Many studies have been focused on an improvement of the flexibility of PLA by blending with tougher polymers such as poly(butylene adipate-co- terephthalate) (PBAT) (Jiang, Wolcott &

Zhang, 2006), poly(butylene succinate) (PBS) (Yokohara &Yamaguchi, 2008), poly (ethylene oxide) (PEO) (Nijenhuis et al., 1996) and natural rubber (NR) (Suksut & Deeprasertkul, 2011) which are also biodegradable polymers. Plasticizers with low molecular weight such as poly(ethylene glycol) (PEG) (Hu et al., 2003), poly(propylene glycol) (PPG) (Piorkowska et al., 2006) and citrate ester (Labrecque et al., 1997) are also successfully improved the mechanical brittleness of PLA. To retain biodegradability property of PLA, many attempts have been made by blending PLA with bio-based plasticizers deriving from renewable plants. Clove essential oil (CLO) (Arfat et al., 2018), epoxidized vegetable oil-based plasticizer, such as epoxidized soybean oil (ESO) (Ali et al., 2009) and epoxidized palm oil (EPO) (Al-Mulla, Suhail & Aowda, 2011), is employed as a feasible alternative. These bio-plasticizer are derived from the renewable source and produced in large quantities at a competitive cost. Therefore, they are attractive raw materials for many industrial applications.

However, the plasticization of PLA always accompanies by a reduction in the strength and stiffness, which is limited with some applications. Reinforcement of PLA with nanofillers is employed to preserve the strength and stiffness of plasticized PLA (Chieng et al. 2015). The addition of nanofillers such as layered silicate clay (Al-Mulla, Suhail & Aowda, 2011), nanocellulose (Meng et al., 2018) and graphene (Arfat et al., 2018; Chieng et al. 2015; Sriprachuabwong et al., 2015) has been reported to improve the mechanical and thermal properties because of their fine dispersion with enormous specific surface area and aspect ratio. A combination of nanoparticle and bio-based plasticizer could make better mechanical and thermal properties of PLA matrix. Plasticizer and nanoparticles strongly influence the morphology developed during the processing, thus the resulting mechanical properties. Because of its superior property improvements of polymers in the previous work, even at very low contents, graphene is an attractive choice to use as a third component in this research work.

Objectives

The aim of this work is to focus on the influence of GP on the plasticized PLA morphology, which is controlled by crystallization, as well as on the correlation between the resulting morphology of composite and its mechanical properties.

Materials and Methods

A commercial grade polylactic acid (PLA) (Luminy L130) was obtained from PURAC (Thailand) Ltd, and prior to use, the PLA was dried overnight at 60°C. Epoxidized soil bean (ESO)

was provided by Srithepthai Chemical co. Ltd. and used as plasticizer. Graphene powder was supported by Haydale Technologies (Thailand).

The PLA was mixed with various content of ESO (3, 5 and 10 wt%) in an internal mixer (MX500, Chareon Tut) with a rotor speed of 60 rpm at 180°C. Beyond 10 wt% ESO content, the PLA/ESO mixture was a powder-like material and it could not be used in the further process. The PLA/ESO mixtures were then extruded using a co-rotating twin screw extruder (CTED22L32, Chareon Tut) with a screw speed of 60 rpm at the die temperature of 180°C. Compression molding (PR2D-W300L350-PM-WCL-HMI, Chareon Tut) was used to prepare the testing samples. With the best mechanical properties, the optimum PLA/ESO blend was chosen to add the GP into the blend using the same procedures as PLA/ESO blends preparation.

Melt flow index (MFI) of neat PLA and PLA/ESO blends was performed according to ASTM standard D1238 using melt flow indexer (MP1200, Tinius Olsen) with a weight of 2.16 kg at 210°C.

Tensile testing was carried out according to ASTM D638 using a universal testing machine (UTM, Model 25ST, Tinius Olsen) with a load cell of 5 kN and a crosshead speed of 5 mm/min. Notched Izod impact testing was accomplished according to ASTM D256 using an impact testing machine (IT504, Tinius Olsen) with a pendulum energy of 5.64 Jules.

Differential scanning calorimetry (DSC, Q200, TA INSTRUMENTS) equipped with the Refrigerated Cooling Systems 90 (RCS90) was used to examined the thermal properties of samples. A weight of sample between 5 to 10 mg was placed in an aluminium pan and the pan was covered by the lid. For the first heating scan, the sample was melted from 0°C to 210°C at 20°C/min and kept isothermal for 5 minutes to erase previous processing history. It was then first cooled from 210°C to 0°C at 10°C/min. The second heating and cooling scans was then performed at the same heating and cooling rates. The degree of crystallinity (X_c) of samples was computed by the following equation:

$$X_C = \frac{100(\Delta H_m - \Delta H_{cc})/\Delta H_m^{\circ}}{\emptyset_{PLA}}$$

where ΔH_m and ΔH_{cc} are the apparent melting and cold crystallization enthalpies of PLA, respectively. ΔH_m° is the the melting enthalpy of a 100% crystalline PLA which is 93.0 J/g (Tsuji & Ikada, 1996) and $\emptyset_{PLA}$ is the weight fraction of PLA in the blends.

The polarized optical microscope (POM, DM2700M, Leica) combined with a heating stage (LTS420, LINKAM) was used to examine the spherulitic structure of samples. A thin section of 10

micrometers of samples was cut from the center of tensile samples using a rotary microtome. The thin section was placed onto a glass slide and covered with a cover slip, then moved to the heating stage. The thin section was melted from 40°C to 210°C with a heating rate of 20°C/min, kept constant at that temperature for 5 minutes. Then, the section was cooled with a cooling rate of 40°C/min to 130°C and held isothermal until crystallization was completed.

Results and Discussion

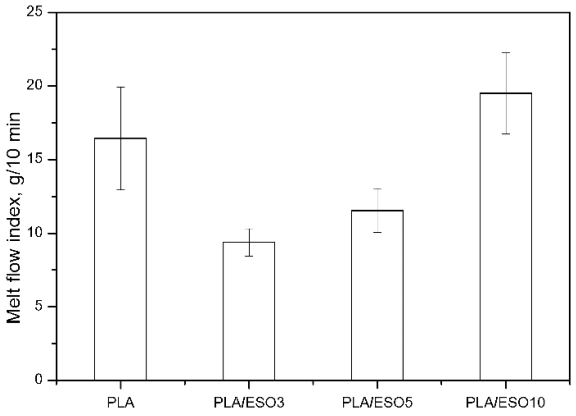

Figure 1 Melt flow index of PLA/ESO blends

The resistance of molten polymer flow is usually identified by the melt flow index (MFI). Figure 1 illustrates the melt flow index of the PLA as a function of plasticizer content. The MFI values decrease as the content of ESO increased up to 5 wt%, which implies that the resistance of PLA molecular flowing is restricted by the ESO segments. Beyond 5 wt% of ESO, the MFI value of PLA/ESO10 is higher compared to neat PLA, which refers to the low viscosity of melt and leads to the lower resistance of melt flow. This is because of the plasticization effect of ESO, which reduces the number of loose attachments between the polymer chains such as van der Waals forces or crystalline structures (Wypych, 2012). The plasticizer separates the polymer chain, allowing the polymer molecules to move more freely, and causes increased polymer chain mobility.

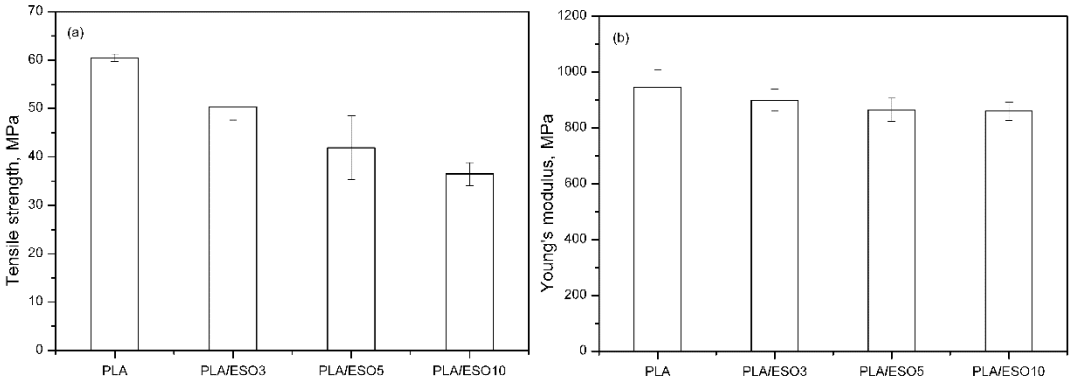

Figure 2 Tensile strength at yield (a) and Young's modulus (b) of PLA/ESO blends

Figure 2 shows the results from tensile testing of neat PLA and PLA/ESO blends. Neat PLA exhibits a tensile strength of about 60 MPa and a Young's modulus of approximately 950 MPa. The tensile strength of PLA reduces with the content of ESO. The tensile strength and the modulus of plasticized PLA lose about 42% and 10%, respectively, of their initial value with 10 wt% of ESO. The deterioration in both tensile strength and Young's modulus is an indication of the plasticizing effect of ESO, which causes by the segmental mobility of PLA chains.

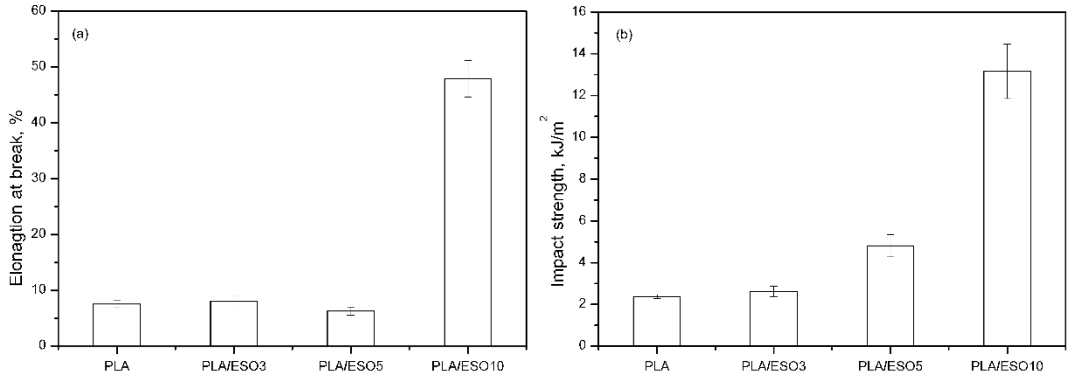

Figure 3 Elongation at break (left) and impact strength (right) of PLA/ESO blends

Figure 3 presents the elongation at break and the impact strength of neat PLA and PLA/ESO blends. Neat PLA provides an elongation at break of 8%. It increases with the presence of ESO, which exhibits the maximum elongation at break (47%) with 10 wt% of ESO. As seen, an impact strength of PLA/ESO blends also increases with content of ESO. An enhancement of the elongation at break and the impact strength is approximately 8 and 5 times of their initial value with

10 wt% of ESO, respectively. Based on the tensile and impact properties, it can deduce that the optimum loading of ESO is 10 wt%, which provides the highest flexibility and impact strength. The presence of ESO lowers the strength of intermolecular forces between PLA molecules by impeding chain-to-chain interactions, thus result in the flexible regions within the samples (Arfat et al., 2018).

Figure 4 illustrates the DSC thermograms of all materials resulted from first cooling scan (a) and second heating scan (b). One can observe glass transition, crystallization, cold crystallization and melting temperatures in the thermograms, which is abbreviated in T_g, T_c, T_{cc} and T_m, respectively. All observed DCS parameters are presented in Table 1. It can be noticed that a single T_g of PLA/ESO10 occurred at a lower temperature as compared to neat PLA, which decreases from 72.3^{O}C of neat PLA to 63.0^{O}C for PLA/ESO10. This reduction in T_g is an evidence of the extent of the plasticizing effect obtained from ESO as plasticizer. But, there is no significant reduction in T_g with the addition GP.

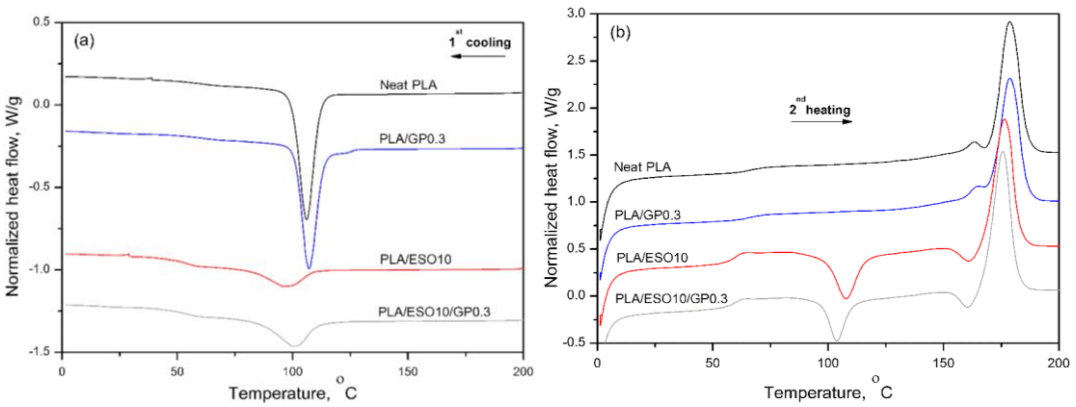

Figure 4 Thermal properties of PLA/ESO/GP nanocomposites: (a) first cooling scan (b) second heating scan

It can also be recognized from the DSC thermograms that the T_c of PLA slightly increases with the addition of GP, which suggest that GP facilitates the PLA chain ability to crystallize. In contrast, the T_{cc} of PLA with an incorporation of ESO is lower than that of neat PLA. This indicates that the ability of PLA to crystallize during cooling is more difficult, which is due to the ESO segments hinder the PLA chain mobility caused by the polymer-plasticizer interactions (Wypych, 2012). In addition, the crystallization of PLA/ESO10 and PLA/ESO10/GP0.3 occurs during second heating (cold crystallization) at above the T_g. The exothermic peak of cold crystallization of PLA/ESO is appeared at about 107.9^{O}C, which is higher than that of the PLA/ESO10/GP0.3 (103.9^{O}C). This proves that GP facilitates the ability to cold crystallization of PLA in PLA/ESO

blend. However, the cold crystallization behavior of PLA is not found in both neat PLA and PLA/GP0.3 because the crystallization is already completed during the cooling.

Table 1 Thermal properties of materials

Materials	T_g (^{O}C)	T_c (^{O}C)	T_{cc} (^{O}C)	T_{m1} (^{O}C)	T_{m2} (^{O}C)	X_c (%)
Neat PLA	72.3	106.0	-	163.2	178.7	37.6
PLA/GP0.3	71.9	107.1	-	163.8	178.7	37.4
PLA/ESO10	63.0	96.5	107.9	-	176.5	51.1
PLA/ESO10/GP0.3	62.9	100.5	103.9	-	175.7	58.8

A common double melting peak is observed in neat PLA and PLA/GP0.3. It could be due to the existence of two different crystal structures in the initial sample. But, it is often relevance to annealing process during DSC scans by which less perfect crystals have time to recrystallize and to remelt. It means that the melting peak at higher temperature (T_{m2}) belongs to more perfect crystals than that at lower temperature (T_{m1}) (Sarasua et al., 1998). The melting endotherms (T_{m2}) are observed at 178.7^{O}C for both neat PLA and PLA/GP0.3. It can be observed that the T_m of PLA decreases with the existence of ESO. This implies that ESO made PLA chain to form less perfect crystals. This is in a good agreement with many reports that the T_m of PLA decreases with increasing plasticizer contents (Labrecque et al., 1997; Ali et al., 2009). With the addition of GP, the crystallinity of neat PLA do not change. However, with the incorporation of ESO, a combination of the crystallinity formed during cooling and heating significant increases.

On the one hand, the presence of ESO reduces the glass transition temperature of PLA as a plasticizer, eases long-range chain motion, and promotes the crystallinity. On the other hand, it may serve as an impurity that obstructs the crystallization process (either nucleation or crystal growth) (Meng et al. 2018). The optical micrographs in Figure 5 reveal the spherulitic structure of different samples. It is obvious that the spherulite size of PLA filled with 0.3 wt% GP is smaller compared to neat PLA. When taking into consideration that the dispersion of GP in PLA matrix is in charge for the nucleation site; the higher number of nuclei the smaller spherulite size (He & Inoue, 2003). On the contrary, the spherulite size becomes larger when the PLA blended with 10 wt% ESO in comparison with neat PLA. It could be due to the restrict movement of PLA chain segments caused by the polymer-plasticizer interactions, which involves hydrogen bonds and van der Waals forces (Wypych, 2012). This hinders the formation of nuclei, thus lessens the number of nuclei and leads to larger spherulite size. In addition, when the GP is added into the PLA/ESO, the

spherulite of PLA turns into smaller size in comparison with PLA/ESO. These results are also found in-line with our previous work of PLA/NR filled with talc (Suksut & Deeprasertkul, 2011).

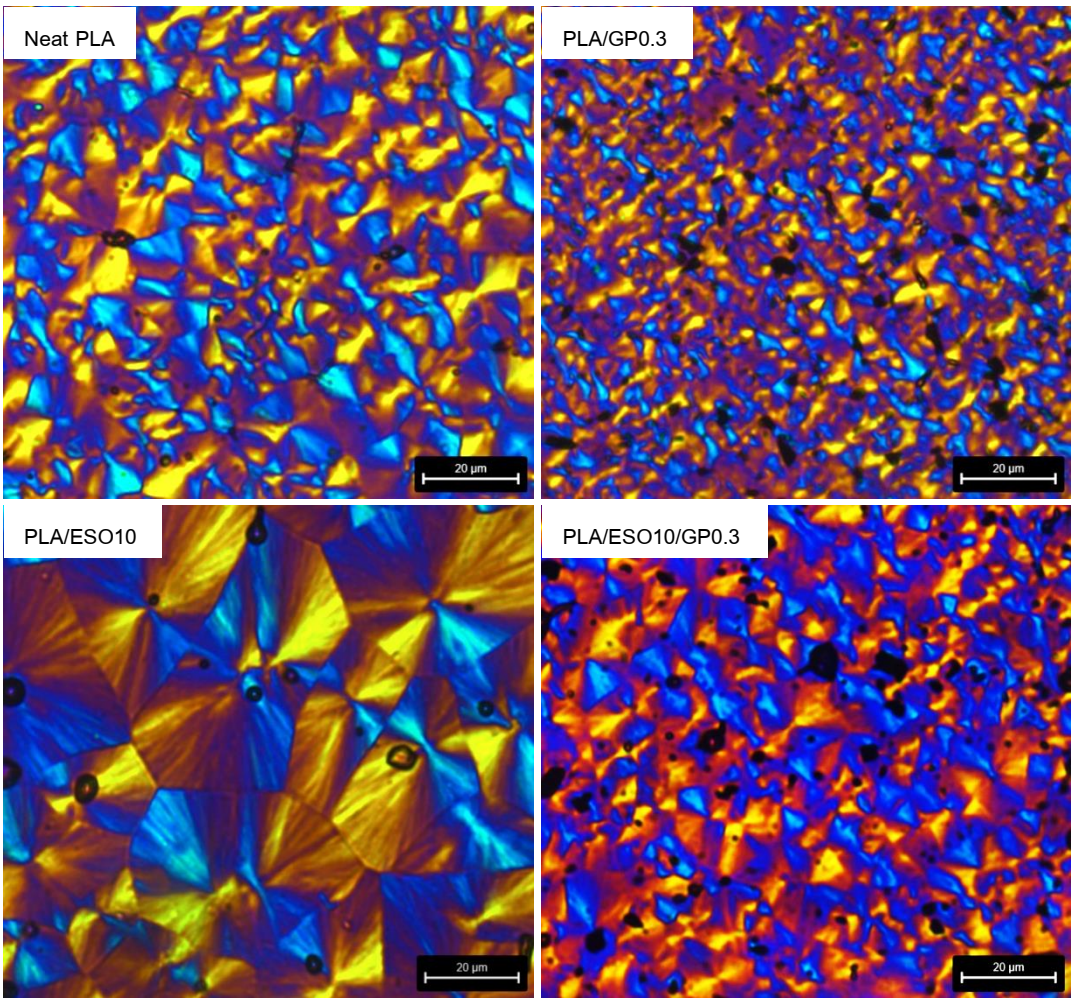

Figure 5 Optical micrographs of the spherulite of PLA/ESO/GP nanocomposites after the completion of crystallization at 130^{O}C.

Tensile properties of PLA and PLA/ESO composites are presented in Figure 6. It can be observed that the tensile strength of neat PLA remains fairly constant with the incorporation of GP. The same trend with a GP is observed in the plasticized PLA composite. However, the Young's modulus of PLA and plasticized PLA drop significantly as the incorporation of GP. As well-known, the mechanical properties of semi-crystalline polymer composite depends on either the reinforcement effect or the crystallization/morphology effect of filler. Higher crystallinity and larger

spherulite size results in a higher strength and stiffness (Popli & Mandelkern, 1987). In addition, an interfacial adhesion between the polymer matrix and the particle filler is an essential key for the reinforcement effect of filler. Although an incorporation of GP into plasticized PLA provides a higher crystallinity as compared to neat PLA, it exhibits no improvement in both strength and stiffness. This could be explained by an insufficient interfacial adhesion between PLA and GP particles (Fu et al., 2008). Therefore, the applied stress cannot be transformed from the PLA matrix to the GP. Not to mention the percolation threshold of GP, at 0.3 wt% of GP loading, the reinforcement effect is not dominant because the amount of filler is not high enough to form a percolated network. It has been reported that the changes in strength and stiffness of the plasticized PLA nanocomposites are attributed by plasticizers and nanofillers. The plasticizers facilitate the chain mobility, and on the other hand, nanofillers impede the mobility of polymer chain (Arfat et al., 2018).

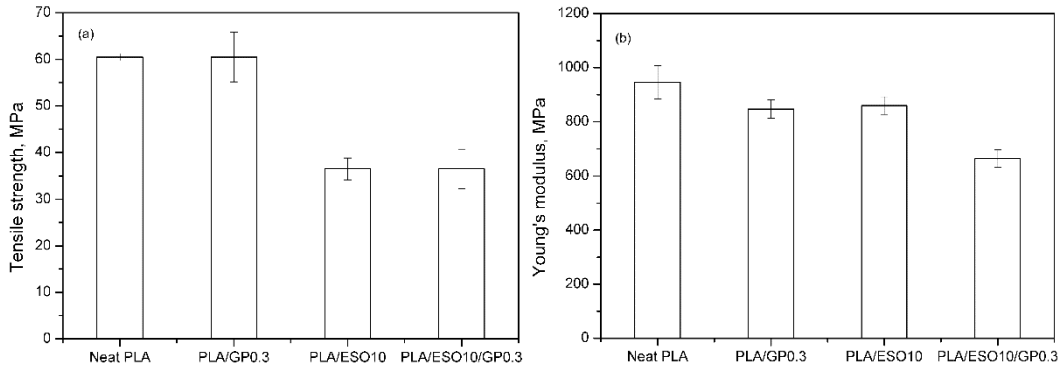

Figure 6 Tensile strength at yield and Young's modulus of PLA/ESO/GP nanocomposites

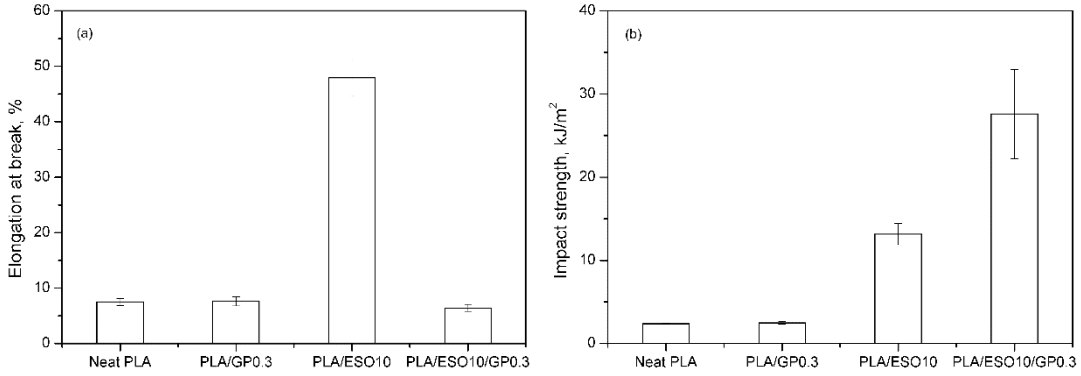

Figure 7 Elongation at break and impact strength of PLA/ESO/GP nanocomposites

The elongation at break of neat PLA has no change with the addition of GP as shown in Figure 7. However, a huge reduction in the elongation at break is observed for PLA/ESO10/GP0.3 as compared to PLA/ESO10. Such a decrease in the elongation at break of PLA/ESO10 with the incorporation of GP despite its relative low Tg is believed to be attributed to a larger aspect ratio of the rigid filler and interaction between GP and PLA/ESO, which obstructs the movement of the polymer chain under the applied stress (Zhao et al., 2010). On the contrary, although the presence of GP in neat PLA does not affect the impact strength, it enhances the impact strength of plasticized PLA about two times as compared to the initial value of PLA/ESO10. As well-known, an impact strength reflects the ability of material absorbing energy when exposed to sudden fracture. The increase in the impact strength could be associated with adhesion between the GP sheets and the PLA/ESO as well as the dispersion state of GP in the PLA/ESO (Chieng, et al., 2012). Based on these results, it suggests that the most likely origin of the improved flexibility in the plasticized PLA composites is the plasticization effect from the ESO, which facilitates the segmental relaxation of PLA. Moreover, the improvement of the impact toughness of plasticized PLA is achieved by the incorporation of GP.

Conclusion

In this work, the ESO plasticized PLA and GP were compounded by melt blending and their mechanical, thermal and morphological properties were investigated. The blending of 10 wt% ESO to the PLA significantly improved the flexibility of PLA, and increased the crystallinity. In the meantime, the presence of GP had less influence on the enhancement of tensile strength, modulus and elongation at break of the plasticized PLA composite. However, the beneficial effect of GP on the impact strength appeared. A thermal and optical studies by DSC and OM, respectively, showed a good nucleating effect of GP in plasticized PLA composite evidenced by lower cold crystallization temperature, higher degree of crystallinity as well as smaller spherulite size as compared to plasticized PLA.

Acknowledgments

This research was funded by King Mongkut's University of Technology North Bangkok. Contract no. KMUTNB-61-NEW-006. The authors gratefully acknowledge Haydale Technologies (Thailand) for supporting the graphene and PURAC (Thailand) Ltd for supporting the polylactic acid. The authors also thank the Srithepthai Chemical co. Ltd. for the supply of the epoxidized soil bean.

References

Al-Mulla, E.A.J., Suhail, A.H. & Aowda, S.A. (2011). New biopolymer nanocomposites based on epoxidized soybean oil plasticized poly(lactic acid)/fatty nitrogen compounds modified clay: Preparation and characterization. *Industrial Crops and Products, 33*(1), 23–29.

Ali, F., Chang, Y.W., Kang, S.C., & Yoon, J.Y. (2009). Thermal, mechanical and rheological properties of poly(lactic acid)/epoxidized soybean oil blends. *Polymer Bulletin, 62*(1), 91–98.

Arfat, Y.A., Ahmed, J., Ejaz, M. & Mullah, M. (2018). Polylactide/graphene oxide nanosheets/clove essential oil composite films for potential food packaging applications. *International Journal of Biological Macromolecules, 107*(PtA), 194–203.

Chieng, B.W., Ibrahim, N.A., Yunus, W.M.Z.W., Hussein, M.Z. & Silverajah, V.S.G. (2012). Graphene nanoplatelets as novel reinforcement filler in poly(lactic acid)/epoxidized palm oil green nanocomposites: Mechanical properties. *International Journal of Molecular Sciences, 13*(9), 10920-10934.

Chieng, B.W., Ibrahim, N.A., Yunus, W.M.Z.W., Hussein, M.Z., Then, Y.Y. & Loo, Y.Y. (2015). Reinforcement of graphene nanoplatelets on plasticized poly(lactic acid) nanocomposites: Mechanical, thermal, morphology, and antibacterial properties. *Journal of Applied Polymer Science, 132*(11), 1-5.

Fu, S.Y., Feng, X.Q., Lauke, B., & Mai Y.W. (2008). Effects of particle size, particle/matrix interface adhesion and particle loading on mechanical properties of particulate-polymer composites. Composites: Part B 39, 933-961.

He, Y. & Inoue, Y. (2003). α-Cyclodextrin-Enhanced Crystallization of Poly(3- Hydroxybutyrate). *Biomacromolecules, 4*(6),1865-1867.

Hu, Y., Hu, Y.S., Topolkaraev, V., Hiltner, A. & Bare, E. (2003). Crystallization and phase separation in blends of high stereoregular poly(lactide) with poly(ethylene glycol). *Polymer, 44*(19), 5681–5689.

Jiang, L., Wolcott, M.P. & Zhang, J. (2006). Study of biodegradable polylactide/poly(butylene adipate-co-terephthalate) blends. *Biomacromolecules, 7*(1), 199-207.

Labrecque, L.V., Kumar, R.A., Davé, V., Gross, R.A. & Mccarthy, S.P. (1997). Citrate Esters as Plasticizers for Poly (lactic acid). *Journal of Applied Polymer Science, 66*(8), 1507–1513.

Meng, X., Bocharova, V., Tekinalp, H., Cheng, S., Kisliuk, A., Sokolov, A. P., Kunc, V. Peter, W. H. & Ozcan, S. (2018). Toughening of nanocelluose/PLA composites via bio-epoxy interaction: Mechanistic study. *Materials and Design, 139*, 188–197.

Nijenhuis, A.J., Colstee, E., Grijpma, D.W. & Pennings, A.J. (1996). High molecular weight poly(-lactide) and poly(ethylene oxide) blends: thermal characterization and physical properties. *Polymer, 37*(26), 5849-5857.

Piorkowska, E., Kulinski, Z., Galeski, A. & Masirek, R. (2006). Plasticization of semicrystalline poly(L-lactide) with poly(propylene glycol). *Polymer, 47*(20), 7178-7188.

Popli, R. & Mandelkern, L. (1987). Influence of structural and morphological factors on the mechanical properties of the polyethylenes. *Journal of Polymer Science: Part B: Polymer Physics, 25*(3), 441-483.

Sarasua, J.R., Prud'homme, R.E., Wisniewski, M., Borgne, A.L. & Spassky, N. (1998). Crystallization and melting behavior of polylactides. *Macromolecules, 31*(12), 3895-3905.

Sriprachuabwong, C., Duangsripat, S., Sajjaanantakul, K., Wisitsoraat, A. & Tuantranont, A. (2015). Electrolytically exfoliated graphene–polylactide-based bioplastic with high elastic performance. *Journal of Applied Polymer Science, 132*(6), 1-8.

Suksut, B. & Deeprasertkul, C. (2011). Effect of nucleating agents on physical properties of poly(lactic acid) and Its blend with natural rubber. *Journal of Polymers and the Environment, 19*(1), 288–296.

Tsuji, H. & Ikada, Y. (1996). Blends of isotactic and atactic poly(lactide)s: 2. Molecular-weight effects of atactic component on crystallization and morphology of equimolar blends from the melt. *Polymer, 37*(4), 595-602.

Wypych, G. (2012). Handbook of Plasticizers (2nd. ed.). Toronto: ChemTec.

Yokohara, T. & Yamaguchi, M. (2008). Structure and properties for biomass-based polyester blends of PLA and PBS. *European Polymer Journal, 44*(3), 677-685.

Zhao, X., Zhang, Q., Chen, D. & Lu, P. (2010). Enhanced mechanical properties of graphene-based poly(vinyl alcohol) composites. *Macromolecules, 43*(5), 2357-2363.

วันที่รับบทความ 16 ธ.ค. 62, วันที่แก้ไขบทความ 6 มี.ค 63, วันที่ตอบรับบทความ 3 เม.ย. 63